Study of Conophylline and Its Inspired Analogues as Potent Pancreatic Lipase Inhibitors for Obesity Treatment

THESIS

Submitted in partial fulfilment

of the requirements for the degree of

DOCTOR OF PHILOSOPHY

by

S N C SRIDHAR

ID. No. 2013PHXF0006P

Under the Supervision of

Dr. Paul Atish Tulshiram

BITS Pilani

Pilani | Dubai | Goa | Hyderabad

BIRLA INSTITUTE OF TECHNOLOGY & SCIENCE, PILANI

2019

Chapter 1 | Introduction

1.1 | Introduction

Overweight and obesity are defined as abnormal or excessive fat accumulation that may impair health [1]. While obesity was earlier considered a metabolic disorder, the World Obesity Federation in 2017, declared obesity as a chronic, relapsing progressive disease process [2]. As of 2016, over 1.9 billion adults (accounting to 39% of the global population) were found overweight, of which 650 million adults were found obese (13% of global population). Overweight and obesity are preliminarily classified using the Body Mass Index [3–5], while Waist-Hip Ratio is considered as a better alternative [6]. The current guidelines suggested by the "American Heart Association/American College of Cardiology/The Obesity Society (AHA/ACC/TOS)" recommends a minimum loss of 500 kcal per day, through physical activity and diet modification to achieve significant weight loss [7]. However, a negative response to life style modification alone, might necessitate either bariatric surgery and/or anti-obesity pharmacotherapy as adjunctive strategies to achieve significant weight loss [8]. Currently, 15 drugs are approved for obesity treatment, that can be further divided under short-term and long-term anti-obesity pharmacotherapy [9,10]. However, a majority of these drugs (with an exception of orlistat and cetilistat) are directed towards reducing the appetite, that would result in an overall inhibition of nutrition intake. On the contrary, orlistat and cetilistat (Fig. 1), act through Pancreatic Lipase (PL) inhibition, an enzyme responsible for the digestion of dietary fats.

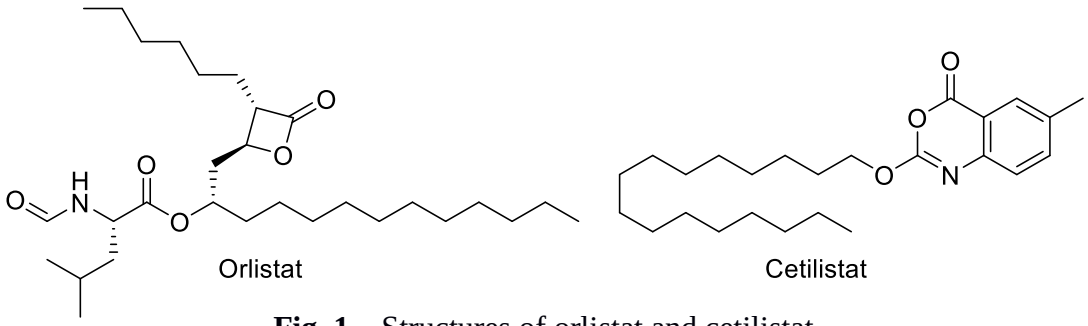

Fig. 1. Structures of orlistat and cetilistat

1.2 | Problem Statement

Orlistat was considered an effective medication, since its approval in 1998 by the United States Food and Drug Administration, and exhibited tolerable side effects *viz.*, steatorrhea, oily stools, frequent or urgent bowel movements [11]. However, recent decade, since 2010, has seen

considerable reports on the severe adverse effects produced by chronic administration of orlistat, including hepatotoxicity, kidney stones, gall stones, liver injury and pancreatitis [12]. Cetilistat, on the other hand, has successfully completed its phase III clinical trial, and has been approved for the treatment of obesity with complications, by the Japanese Ministry of Health, Family and Welfare on September 20, 2013 [13]. However, the drug has not been approved by the FDA to date. The scenario clearly highlighted the urgent need for safer and effective PL inhibitors for the treatment of obesity.

Chapter 2 | Literature Review

2.1 | Literature Review

Natural products (NPs) represent a vast reservoir of chemical entities and have been an effective source for the treatment of various disorders and diseases, while producing lesser adverse effects [14]. Considering the advantages of NP-based drug discovery, a detailed literature search was performed to identify NP-based PL inhibitors, that in turn would provide structural features required for potent PL inhibition. Apart from, various synthetic PL inhibitors were also reviewed. The search highlighted around 750 NPs, that can be further classified under diverse chemical classes *viz.*, polyphenols, saponins, triterpenes and alkaloids etc. Of these, polyphenols comprise the major class of PL inhibitors followed by saponins, while the other classes can be considered minor. Similarly, around 300 synthetic PL inhibitors have been identified and include boronic acids, alkyl phosphonates, α-ketoamides, squaric acid derivatives, oxadiazolones, chalcones, benzylisoquinolines, bisbenzimidazoles and triazoles etc. Nevertheless, a majority of these compounds did not possess potential PL inhibitory activity comparable to orlistat.

2.2 | Gaps in existing research

The literature review has resulted in identification of around 750 NP-based PL inhibitors apart from 300 synthetic PL inhibitors. However, the following gaps were identified in the existing research.

- Vast chemical diversity in the existing literature, with minimum efforts to understand the structural features for potent PL inhibition.
- Negligible use of *in silico* techniques to understand the requirement of molecular interactions with the active site

- Few attempts that involve structural modifications to the existing NPs to enhance their PL inhibitory potential

Chapter 3 | Aim and Objectives

Considering the potential gaps in the existing research, the present thesis aims at ***"the study of NP lead(s) and its inspired analogues as potent PL inhibitors for obesity treatment".***

To achieve the above aim, following studies were set as objectives;

1. To prepare extracts from selected Indian medicinal plants and determine their *in vitro* PL inhibitory activity
2. To perform bioassay guided fractionation of the most potent extract followed by purification and characterization of the isolated NP lead(s)
3. To evaluate the NP lead(s) for *in vitro* PL inhibition and identify the structural features required for activity using *in silico* methods
4. To design, synthesise and evaluate various analogues of NPs lead for their PL inhibitory activity.
5. To evaluate the *in vivo* efficacy of the most potent synthetic analogue using High Fat Diet (HFD) fed mice model

Chapter 4 | Materials and Methods

4.1 | Plant material collection, processing and extraction

Plant materials were either collected from BITS Pilani (located at 28.36°N 75.58°E and 285 m above the sea level) or procured from commercial suppliers and authenticated by a qualified botanist. The plant materials were shade dried, powdered, sieved and subjected to sequential extraction using hexane and methanol with the aid of three extraction techniques; Cold Maceration (CM) for 72 h at RT, Hot Percolation (HP) for 24 h at 40-60°C and Ultrasonic assisted Extraction (UE) for 1 h at 25-30°C.

4.2 | PL inhibition assay and enzyme kinetics

The procedure for PL inhibition assay was performed as per the previously reported literature with minor modifications [15]. Briefly, the reaction mixture comprised of 875 µL of Tris buffer (pH - 7.4), 100 µL of enzyme solution (5 mg/mL) and 20 µL of the inhibitor of various stock concentrations, pre-incubated for 5 min at 37°C, followed by addition of 10 µL of the substrate (4-nitrophenyl butyrate, 10 mM in acetonitrile). The absorbance of the final

mixture was taken after 5 min at an absorbance maximum of 4-nitrophenol (405 nm), to calculate the % inhibition and IC_{50}. For the inhibition kinetics, the assay protocol was repeated at four different concentrations of substrate and increasing concentrations of the inhibitor. A double reciprocal Lineweaver-Burk plot with reciprocals of reaction velocity and substrate concentration (on y-axis and x-axis, respectively) were plotted to understand the nature of inhibition [16]. The inhibition constant, K_i, was calculated using Cheng-Prusoff equation [17].

4.3 | Molecular Docking and Molecular Dynamics simulations

Molecular docking studies were performed with the aid of Molegro Virtual Docker 6.0 (CLC Bio, Denmark), and the crystal structure of the open lid conformation of the Human PL was retrieved from the RCSB Protein Data Bank (PDB Code: 1LPB) [18,19]. The ligands were energy minimised using Molecular Mechanics 2 (MM2) force field in Chem3D module of ChemBioOffice (PerkinElmer, USA) and subjected to docking on validated grid parameters. The obtained docked poses of the ligands were analysed for their MolDock scores, while the various interactions exhibited by the ligands with the active site were visualised in Discovery Studio Visualizer (Dassault Systemes Biovia, USA).

Molecular dynamics (MD) was performed for the most potent ligands using GROningen Machine for Chemical Simulations (GROMACS 5.0.4), compiled on a CentOS 7 operating system equipped with Intel(R) Xeon(R) CPU W3565 and NVIDIA Quadro 4000 Quad-Core Processor. CHARMM27 force field was applied during the MD run [20], Prior to the initiation of the MD, the complex was minimized using Steepest Descent algorithm, followed by system stabilization using the canonical NVT and NPT ensembles.

Chapter 5 | Identification of NP Lead from *T. divaricata* and Its Validation

A detailed literature review has resulted in the identification of various structural features *viz.*, a) large molecular volume that can be able to interact with the active site as well as the hydrophobic lid domain; b) presence of an ester or ester mimicking group with a reactive carbonyl functionality that would interact with Ser152 of the active site. Consequently, a pool of 20 Indian medicinal plants/parts were selected based on above information and hints from traditional medicines. These were screened using the PL inhibition assay, wherein the methanol extract obtained through ultrasonic extraction of *Tabernaemontana divaricata* leaves exhibited comparatively greater potential (IC_{50} = 12.73 µg/mL). Phytochemically, the leaves of *T. divaricata* are a rich source of indole alkaloids apart from various other classes of minor

chemical constituents. Considering the effect of seasons on the metabolic profile of plants which in turn can result in varied pharmacological activity [21,22], the leaves of *T. divaricata* were collected every trimester over a period of one year *i.e.*, during the 15th day of November 2013, February 2014, May 2014 and August 2014. The methanol extracts these samples were subjected to PL inhibition assay, that highlighted the August 2014 sample to possess greater potent (IC_{50} = 9.26 µg/mL).

Consequently, the leaves were collected in large scale during August 2014, processed and subjected to exhaustive ultrasonic extraction with hexane and methanol. The obtained methanol extract was subjected to bioassay guided fractionation, that ultimately resulted in the isolation and identification of conophylline as a NP lead with potential PL inhibition. Conophylline, a bis-indole alkaloid, exhibited an IC_{50} of 3.31 µM while orlistat exhibited an IC_{50} of 0.99 µM. Moreover, enzyme kinetics of conophylline and orlistat indicated that both the compounds exhibited a reversible competitive inhibition. The potency of conophylline was also validated by molecular docking and molecular dynamics, wherein conophylline as well as two other bis-indole alkaloids, conophyllinine and conophyllidine exhibited potential MolDock score of -143.382, -137.553 and -133.011 kcal/mol respectively, while the monomeric counterpart of these alkaloids, taberhanine exhibited a low score of -113.252 kcal/mol (Fig. 2).

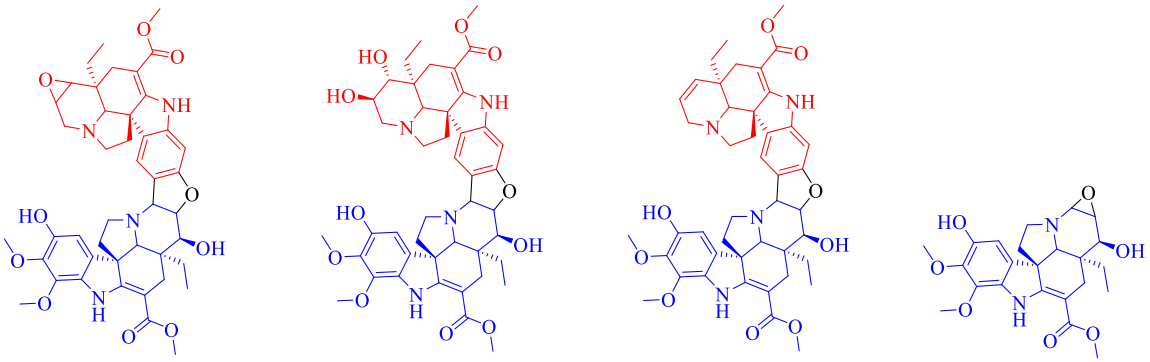

Fig. 2. Structures of Conophylline, Conophyllinine, Conophyllidine and Taberhanine

Further, a 10 ns molecular dynamics (MD) simulation of these four molecules indicated a stable binding conformation (RMSD < 1 Å) for the bis-indoles aided through strong hydrophobic interactions with the lid domain of Human PL. This was not observed in case of taberhanine.

Considering the potential role of conophylline in PL inhibition, it was quantified in 12 alkaloid rich fractions (ARFs) obtained from four leaf samples subjected to three extraction

techniques. Prior to quantification, a HPTLC method was developed and validated as per the Q2 (R1) guidelines of International Conference on Harmonization (ICH). Conophylline yield was highest in samples collected in August 2014, followed by November 2013, February 2014, and least during May 2014. Further, the extractive yield of conophylline was high with ultrasonic extraction, followed by hot percolation and cold maceration (Fig. 3). Moreover, the PL inhibitory activity of the 12 ARF samples exhibited significant correlation to their respective conophylline content ($p < 0.05$, Pearson's r = -0.7152, r^2 = 0.5115; calculated using Pearson Correlation Analysis), clearly indicating conophylline as a potential PL inhibitory NP lead from *T. divaricata.*

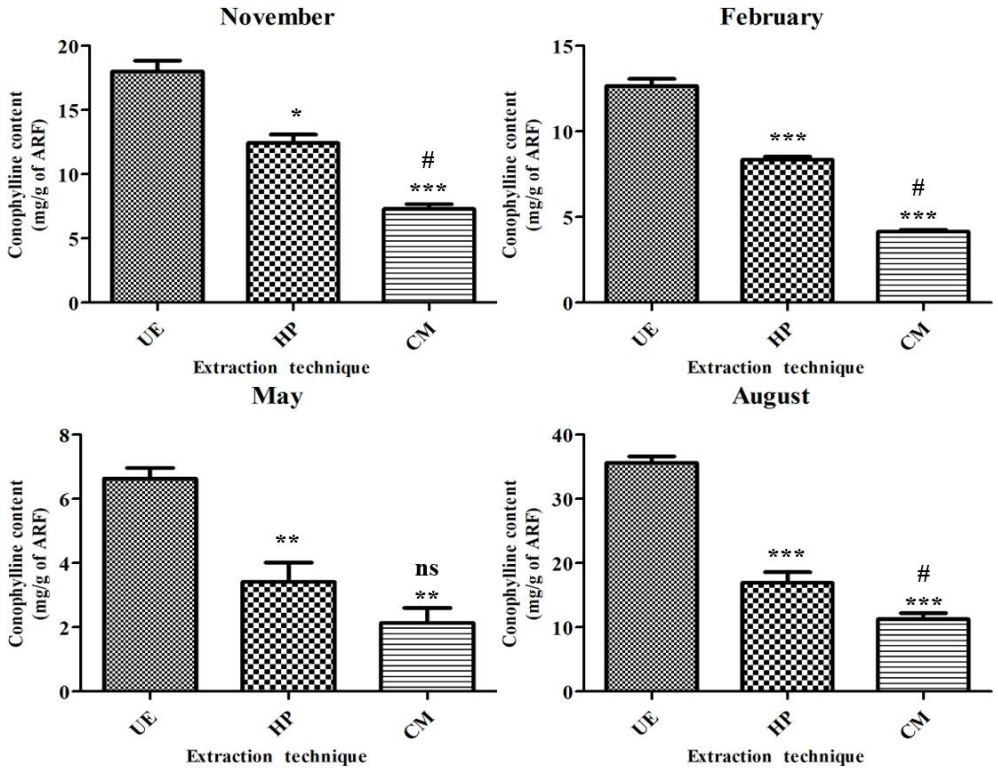

Fig. 3. Extractive yields of conophylline (mg/g) in different ARF Samples. All the values were represented as mean ± SEM (n=3). **November** - $^{*}p < 0.05$ *Vs.* UE, $^{***}p < 0.001$ *Vs.* UE, $^{\#}p < 0.01$ *Vs.* HP; **February** - $^{***}p < 0.001$ *Vs.* UE, $^{\#}p < 0.001$ *Vs.* HP; **May** - $^{**}p < 0.01$ *Vs.* UE, ns – not significant *Vs.* HP; **August** - $^{***}p < 0.001$ *Vs.* UE, $^{\#}p < 0.05$ *Vs.* HP. (UE – Ultrasonic extraction; HP – Hot percolation; CM – Cold maceration)

Chapter 6 | Synthesis - Series I - Carbazolyl Oxoacetamide Analogues

Conophylline exhibited a potential PL inhibition, however, was significantly lower compared to orlistat. An *in-silico* analysis of conophylline in the active site of Human PL highlighted a high degree of unfavourable steric interactions. Further, conophylline lacked a reactive ester group, a structural feature that would interact with the Ser152 of the active site. The fact can be further confirmed with the previous literature, wherein the carbazole alkaloids *viz.*, mahanimbine and koenimbin, possessed potential to poor PL inhibitory activity and did not contain an ester or ester mimicking group essential for potential PL inhibition [23]. Scaffolds including fluorinated ketones, α-keto esters, α-ketoamides and 1,2-diketones have been found to possess reactive carbonyl groups that act as an electrophile for Ser152 [24,25]. Further, the role of α-ketoamides as an ester mimicking group was previously described, where the replacement of ester with ketoamide in the triacylglycerol analogues led to potential PL inhibition [26–28]. Based on the above findings, we hypothesized the carbazolyl oxoacetamide analogues to possess potential PL inhibitory activity (Fig. 4). These carbazolyl oxoacetamides can be considered a pharmacophore hybrid of the carbazole scaffold (present in conophylline) and α-ketoamide functionality, present in a single molecule.

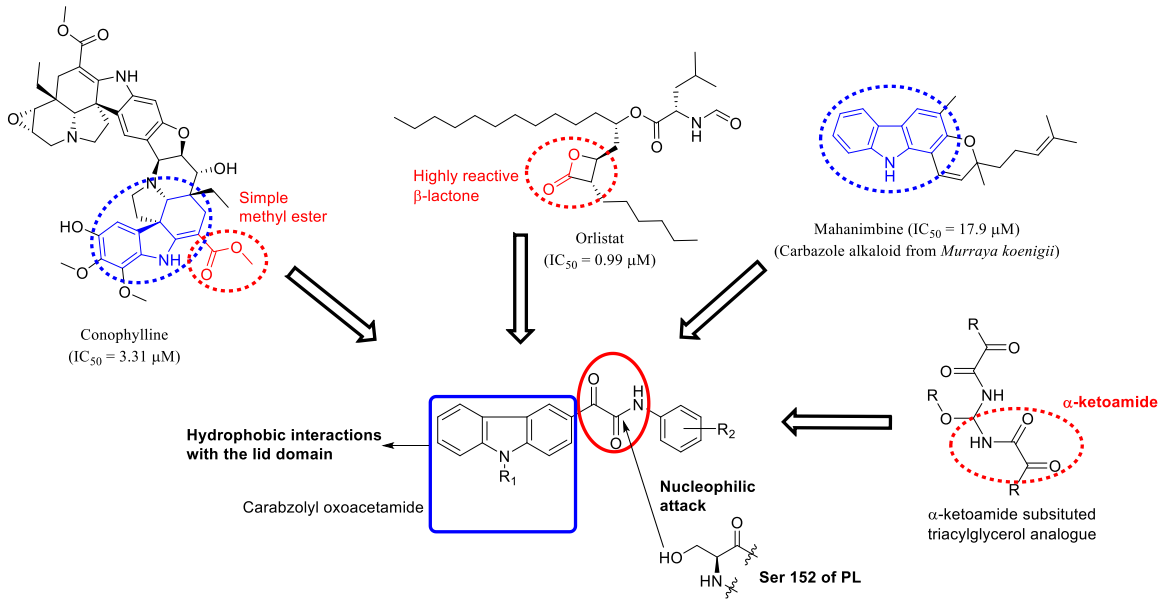

Fig. 4. Rationale for selecting carbazolyl oxoacetamide analogues as PL inhibitors

In total, a series of 24 carbazolyl oxoacetamide analogues (**DK-1** to **DK-24**) were synthesized and evaluated for their PL inhibitory activity. The analogues were characterised by spectroscopic techniques. In the series **DK-5** exhibited the most potent activity against PL, with

an IC_{50} of 6.31 µM, followed by **DK-6** and **DK-16** with 8.72 and 9.58 µM, respectively (Fig. 5). Further, these compounds exhibited a reversible competitive inhibition similar to orlistat and conophylline. A preliminary structure-activity relationship of the carbazolyl oxoacetamide analogues indicated that the presence of aromatic benzyl group on the carbazolyl nitrogen increased the PL inhibition activity of analogues. Similarly, the presence of an electron-donating group on the amide nitrogen potentiated the PL inhibitory activity of the analogues (Fig. 6). Molecular docking studies validated the rationale for selecting the carbazolyl oxoacetamide analogues wherein the carbazole scaffold exhibited hydrophobic interactions with the lid domain, while the reactive carbonyl group of the α-ketoamide existed near to Ser152 of the active site. Further, molecular modelling studies indicated the absence of any unfavourable steric bumps with **DK-5**, in contrast to conophylline. Moreover, most of the ligands exhibited an additional π-cation interaction with Arg 256, an amino acid that plays a key role in the opening of the lid domain. A 10 ns MD simulation performed for **DK-5** in complex with PL, indicated stable binding conformation of the ligand in the active site (maximum RMSD of 4 Å, recorded from 8-10 ns).

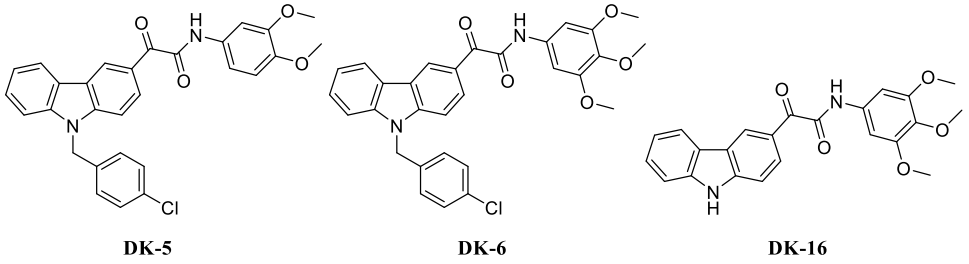

Fig. 5. Structures of the carbazolyl oxoacetamide analogues **DK-5, DK-6** and **DK-16**

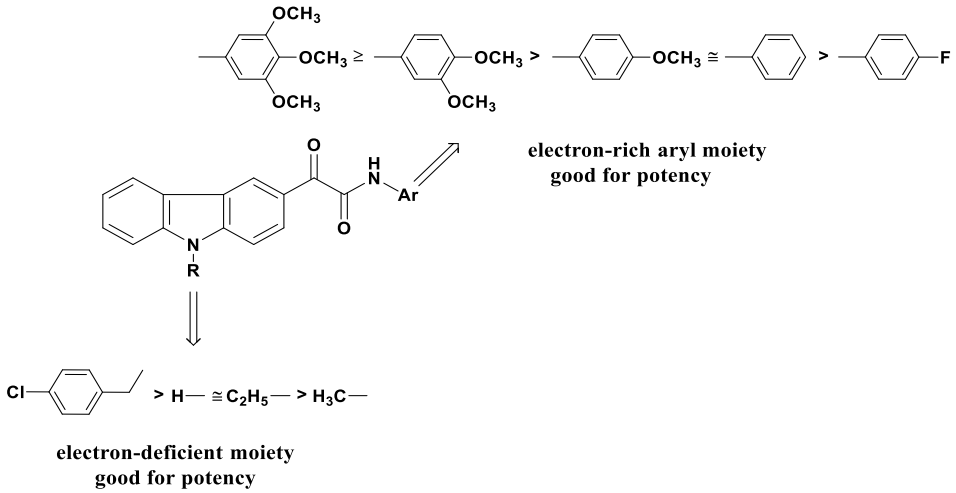

Fig. 6. Preliminary structure-activity relationship of the carbazolyl oxoacetamide analogues

Chapter 7 | Synthesis - Series II - Indolyl Oxoacetamides Analogues (Part 1)

Compound **DK-5** from the carbazolyl oxoacetamide analogues series exhibited a potential PL inhibition with an IC_{50} value of 6.31 µM. Nevertheless, a lower PL inhibitory potential of **DK-5** compared to conophylline (IC_{50} = 3.31 µM) can be attributed to three drawbacks, as determined through *in silico* analysis of the docking poses of orlistat, conophylline and **DK-5;** i) A greater interaction distance between the reactive carbonyl group of the ketoamide and Ser152 of the active site; ii) A lesser intensity of hydrophobic interactions exhibited by **DK-5** in comparison to conophylline and orlistat and iii) the strength of the π-cation interaction with Arg 256 (Fig. 7).

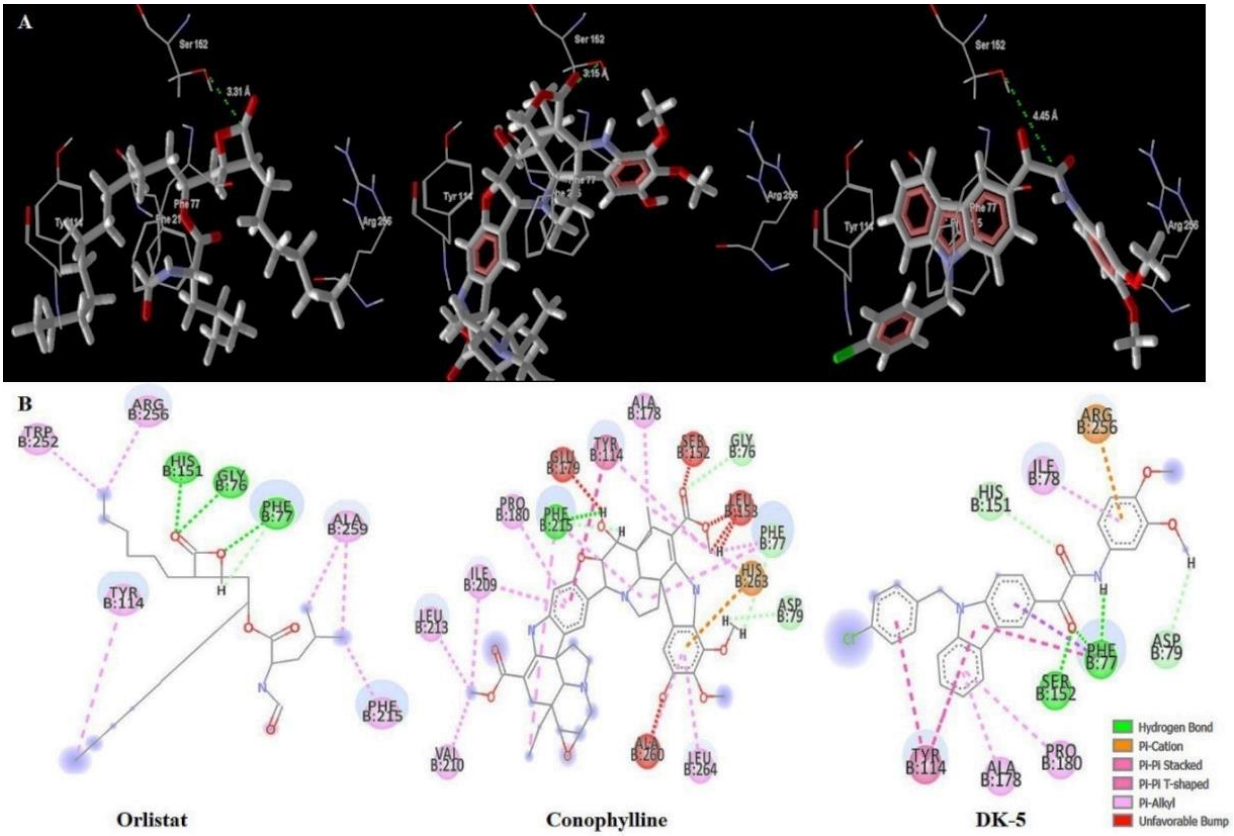

Fig. 7. (A) 3D poses of orlistat, conophylline and **DK-5** highlighting the distance of reactive carbonyl from Ser152 (3.31, 3.15 and 4.45 Å, respectively); **(B)** 2D interactions highlighting no unfavourable steric bumps and low degree of hydrophobic interactions in **DK-5**.

The first drawback was rectified by replacing the carbazole scaffold with an indole scaffold that resulted in significant reduction in the steric hinderance as well as the interaction distance as confirmed by preliminary docking study. Consequently, a series of 39 indolyl oxoacetamide analogues (**AP-1** to **AP-39**) were synthesized, characterised and evaluated for their PL inhibitory potential. Compound **AP-37** exhibited the most potent activity against PL, with an IC_{50} of 4.53 µM, followed by **AP-21**, **AP-36** and **AP-35** with IC_{50} of 4.92, 5.12 µM and 6.28 µM, respectively (Fig. 8). Further, enzyme kinetics study for **AP-21, AP-36** and **AP-37** indicated reversible competitive inhibition similar to carbazolyl oxoacetamide analogues. The PL inhibitory activity of the indolyl oxoacetamide analogues **AP-1** to **AP-39** indicated a similar structure activity relationship as observed with the carbazolyl oxoacetamide analogues. As represented in Fig. 9, the presence of aromatic benzyl group on the indole significantly increased the PL inhibitory activity of analogues in comparison to the ethyl substitution and the unsubstituted counterparts. Similarly, the presence of ring activating groups on the aryl ring of the amide nitrogen resulted in better potency of the analogues. Moreover, the presence of a methylene bridge between the aryl extension and the amide nitrogen resulted in potent activity. The MolDock scores of these analogues were in agreement to their PL inhibitory profile wherein **AP-37,** the most active compound from the series possessed a top docking score of -163.052 kcal/mol. In addition, *in silico* studies also validated the importance of π-cation interaction with Arg 256 and its enhancement with ring activating groups. Compound **AP-37** exhibited a stable binding conformation (RMSD < 2 Å) throughout the 10 ns MD simulation.

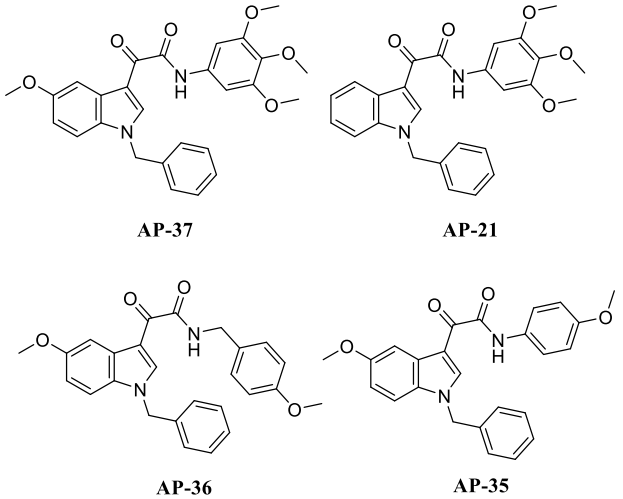

Fig. 8. Chemical structures of the indolyl oxoacetamide analogues **AP-37, AP-21, AP-36** and **AP-35**

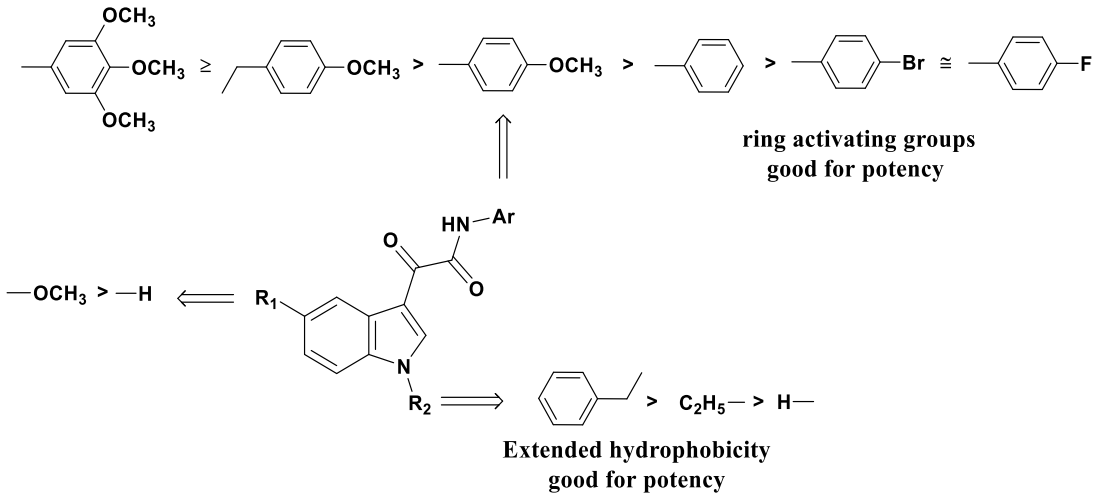

Fig. 9. Structure-activity relationship for indolyl oxoacetamide analogues **AP-1** to **AP-39**

Chapter 8 | Synthesis - Series III - Indolyl Oxoacetamide Analogues (Part 2)

The first series of indolyl oxoacetamide analogues has validated the hypothesis of replacing carbazole with an indole nucleus that resulted in significant enhancement in the PL inhibitory potential. Nevertheless, **AP-37** that possessed a 5-methoxy substitution on the indole, did not exhibit significantly potent activity compared to its unsubstituted counterpart, **AP-21** (IC_{50} = 4.92 µM), clearly indicating its negligible role in the activity. The lower potency of these analogues compared to conophylline can be attributed to the low hydrophobic density on the indole scaffold. Further, the presence of a -CH_2 linker between the aryl extension and the amide as observed with **AP-36** resulted in enhanced potential (5.12 µM) compared to its counterpart, **AP-35** (6.28 µM), that did not possess the linker.

Considering these facts, the second part is focussed on further structural optimization of the indolyl oxoacetamide analogues with the following inclusions, i.e., i) enhancement of the hydrophobic density on the indole nucleus and ii) optimization of the aryl extension on the amide for better π-cation interaction with Arg256. Accordingly, the following substitutions were included, *viz.*,

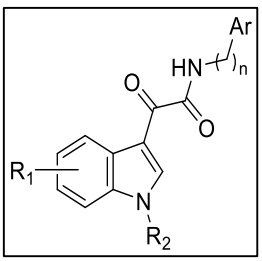

i) An additional aromatic substitution on the benzene ring of the indole (**R_1**); ii) Dense lipophilic groups, such as prenyl and geranyl moieties on the indole nitrogen (**R_2**) and iii) increasing the carbon linker chain (**n**) and replacing the simple substituted aryl groups on the amide nitrogen (**Ar**) with indole to enhance the π-cation strength with Arg256.

In total, 41 analogues (**SS-1** to **SS-41**) were synthesized and evaluated for their PL inhibitory activity. Compound **SS-39** exhibited potent activity, followed by **SS-40** with IC_{50} values of 1.68 and 2.24 µM, respectively comparable to orlistat (Fig. 10). Apart from, 10 other derivatives from this series exhibited greater potential over the NP lead, conophylline. The study highlighted the C_6 and C_7 positions of the indolyl oxoacetamide analogues favourable for the substitution of aromatic rings, that would result in potential PL inhibition in the presence of a N-geranyl moiety.

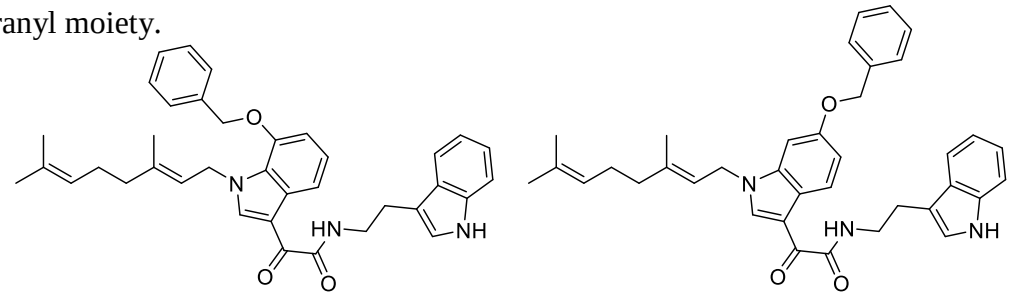

SS-39 **SS-40**

Fig. 10. Chemical structures of the indolyl oxoacetamide analogues **SS-39** and **SS-40**

A general representation of the SAR of the indolyl oxoacetamide analogues **SS-1** to **SS-41** is provided in Fig. 11, and can be attributed to the substitutions at R_1, R_2 and Ar. At R_1, the 7-benzyloxy and 6-benzyloxy substituted indolyl oxoacetamide analogues exhibited greater potency over the 5-benzyloxy and the 4-benzyloxy counterparts. On the other hand, geranyl substitution at R_2 favoured better potency, followed by the prenyl and benzyl substitutions, while ethyl and unsubstituted analogues exhibited significantly lower potency. For the substitution at Ar, the 2-(indol-3-yl)ethyl moiety resulted in a better potency over the trimethoxybenzyl substitution followed by the trimethoxyphenyl substitution.

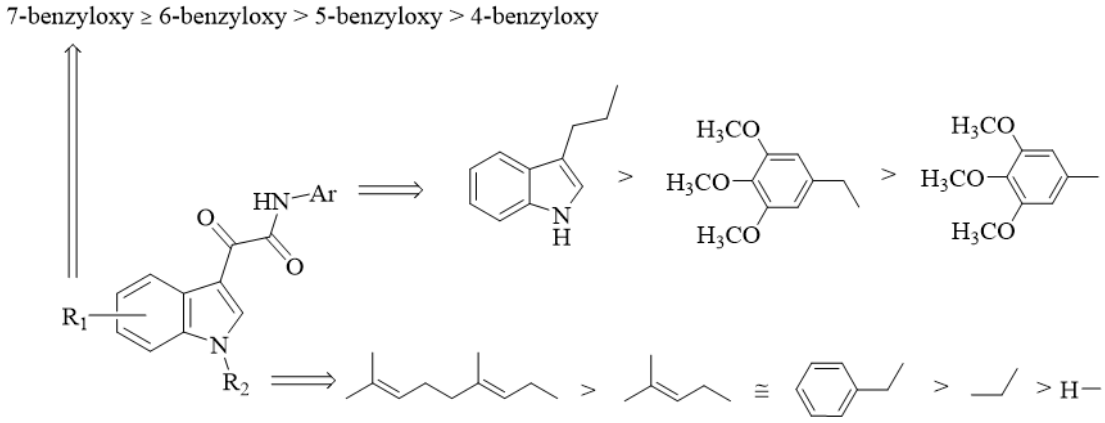

Fig. 11. Structure-activity relationship for indolyl oxoacetamide analogues **SS-1** to **SS-41**

Chapter 9 | ADMET prediction and *in vivo* experiments

The results from the previous chapters (**6-8**) have identified various carbazolyl and indolyl oxoacetamide analogues to exhibit potent PL inhibitory activity. Nevertheless, the *in vivo* efficacy of a given drug is predominantly affected, not only by its *in vitro* potential but also the various pharmacokinetic parameters and the toxicity properties that decide the fate of the drug [29]. Hence the ADMET parameters of the most potent analogues from the previous chapters, that in turn would identify the best candidate to proceed for the *in vivo* experiments. A total of 11 compounds were considered for the ADMET prediction and included the most potential compounds from the DK series, AP series and SS series alongside conophylline (NP Lead) and orlistat (standard). For the DK, AP and SS series, compounds with IC_{50} less than 10 µM, 5 µM and 2.5 µM, respectively were selected. The study highlighted **SS-39** as a suitable candidate for the *in vivo* experiments, as it possessed low GI absorption similar to orlistat, and was devoid of carcinogenicity, oral and liver toxicity in contrary to orlistat.

The *in vivo* experiments were conducted on male Swiss albino mice, and included two studies namely, i) Oral Triglyceride Tolerance Test (OTTT)[30], ii) HFD fed mice model (4-week treatment study)[31]. Compound **SS-39** at 20 mg/kg dose exhibited a similar activity in comparison to 10 mg/kg orlistat (Fig. 12). Further, the quantity of faecal triglycerides in the **SS-39** (20 mg/kg) group was not significantly different in comparison to the orlistat (10 mg/kg) group clearly indicating that **SS-39** acted through PL inhibition.

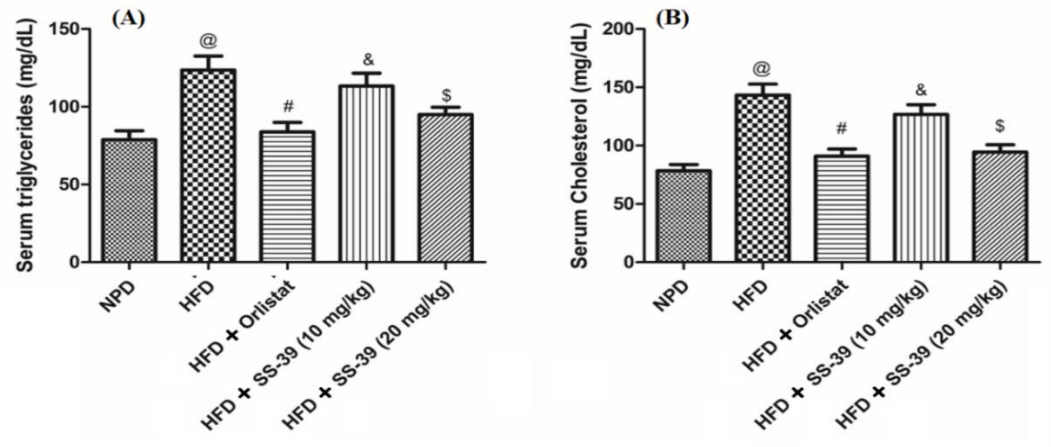

Fig. 12. (A) Serum triglyceride and **(B)** Serum total cholesterol ($^{@}p < 0.001$ *Vs.* NPD; $^{\#}$ns *Vs.* NPD; $^{\&}p < 0.001$ *Vs.* HFD plus Orlistat; $^{\$}$ns *Vs.* HFD plus Orlistat) All the biochemical parameters were determined after the 4-week treatment period and the values are represented as mean ± SEM).

Chapter 10 | Conclusion and future perspectives

The thesis work resulted in a potent indolyl oxoacetamide analogues **SS-39** identified through molecular modelling and bioassay guided structural modifications to conophylline (Fig. 13), wherein the pharmacological efficacy of this compound was significantly similar to the standard, orlistat. Further, **SS-39** did not possess any toxicity in contrary to orlistat, as observed with preliminary ADMET prediction.

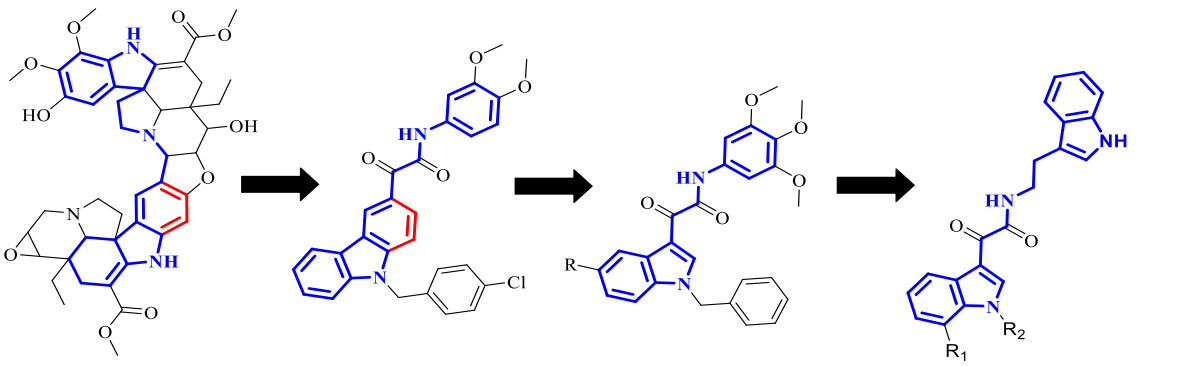

Fig. 13. Schematic flow of structural modifications to conophylline that resulted in potent PL inhibitory bis(indolyl)oxoacetamide **SS-39**

References

[1] http://www.who.int/topics/obesity/en/ (last accessed May 23, 2019).

[2] G.A. Bray, K.K. Kim, J.P.H. Wilding, Obesity: A chronic relapsing progressive disease process. A position statement of the World Obesity Federation, Obes. Rev. 18 (2017) 715–723.

[3] http://www.who.int/mediacentre/factsheets/fs311/en/ (last accessed on 21 May 2019).

[4] http://www.who.int/childgrowth/standards/weight_for_height/en/ (last accessed May 23, 2019).

[5] http://www.who.int/growthref/who2007_bmi_for_age/en/ (last accessed May 23, 2019).

[6] Waist circumference and waist-hip ratio: Report of a WHO expert consultation, Geneva, 8-11 December 2008, ISBN 9789241501491.

[7] M.D. Jensen, D.H. Ryan, C.M. Apovian, J.D. Ard, A.G. Comuzzie, K.A. Donato, F.B. Hu, V.S. Hubbard, J.M. Jakicic, R.F. Kushner, 2013 AHA/ACC/TOS guideline for the management of overweight and obesity in adults: A report of the American college of

Cardiology/American Heart Association Task Force on Practice Guidelines and The Obesity Society, J. Am. Coll. Cardiol. 63 (2014) 2985–3023.

[8] D. Patel, Pharmacotherapy for the management of obesity, Metab. Exp. 64 (2015) 1376–1385.

[9] D. Haslam, Weight management in obesity-past and present, Int. J. Clin. Pract. 70 (2016) 206–217.

[10] S. Manning, A. Pucci, N. Finer, Pharmacotherapy for obesity: Novel agents and paradigms, Ther. Adv. Chronic Dis. 5 (2014) 135–148.

[11] A.M. Heck, J.A. Yanovski, K.A. Calis, Orlistat, a new lipase inhibitor for the management of obesity, Pharmacother. J. Hum. Pharmacol. Drug Ther. 20 (2000) 270–279.

[12] https://wayback.archive-it.org/7993/20170112172652/http://www.fda.gov/Safety/MedWatch/SafetyInformation/ucm215504.htm (last accessed May 23, 2019).

[13] https://www.norgine.com/press_release/norgine-and-takeda-announce-the-new-drug-application-approval-of-oblean-cetilistat-tablets-120mg-in-japan/ (last accessed May 23, 2019).

[14] G.M. Cragg, D.J. Newman, Natural products: A continuing source of novel drug leads, Biochim. Biophys. Acta-General Subj. 1830 (2013) 3670–3695.

[15] Y. Bustanji, I.M. Al-Masri, M. Mohammad, M. Hudaib, K. Tawaha, H. Tarazi, H.S. AlKhatib, Pancreatic lipase inhibition activity of trilactone terpenes of *Ginkgo biloba*, J. Enzyme Inhib. Med. Chem. 26 (2011) 453–459.

[16] H. Lineweaver, D. Burk, The determination of enzyme dissociation constants, J. Am. Chem. Soc. 56 (1934) 658–666.

[17] B.T. Burlingham, T.S. Widlanski, An intuitive look at the relationship of K_i and IC_{50}: A more general use for the Dixon plot, J. Chem. Educ. 80 (2003) 214.

[18] M.P. Egloff, F. Marguet, G. Buono, R. Verger, C. Cambillau, H. van Tilbeurgh, The 2.46 Å resolution structure of the pancreatic lipase-colipase complex inhibited by a C_{11} alkyl phosphonate, Biochemistry. 34 (1995) 2751–2762.

[19] R. Thomsen, M.H. Christensen, MolDock: A new technique for high-accuracy molecular docking, J. Med. Chem. 49 (2006) 3315–3321.

[20] A.D. MacKerell, N. Banavali, N. Foloppe, Development and current status of the CHARMM force field for nucleic acids, Biopolymers. 56 (2000) 257–265.

[21] R.D. Singh, R.L. Meena, B. Sharma, B. Singh, V.K. Kaul, P.S. Ahuja, others, Seasonal variation of bioactive components in *Valeriana jatamansi* from Himachal Pradesh, India, Ind. Crops Prod. 32 (2010) 292–296.

[22] N. Manika, S. Singh, R.K. Verma, G.D. Bagchi, Extraction efficacy, stability assessment and seasonal variation of bioactive 'gymnemagenin'in *Gymnema sylvestre*, Ind. Crops Prod. 44 (2013) 572–576.

[23] R. Birari, S.K. Roy, A. Singh, K.K. Bhutani, Pancreatic lipase inhibitory alkaloids of *Murraya koenigii* leaves, Nat. Prod. Commun. 4 (2009) 1089–1092.

[24] W. Han, Z. Hu, X. Jiang, C.P. Decicco, α-ketoamides, α-ketoesters and α-diketones as HCV NS3 protease inhibitors, Bioorg. Med. Chem. Lett. 10 (2000) 711–713.

[25] C. Steuer, C. Gege, W. Fischl, K.H. Heinonen, R. Bartenschlager, C.D. Klein, Synthesis and biological evaluation of α-ketoamides as inhibitors of the Dengue virus protease with antiviral activity in cell-culture, Bioorg. Med. Chem. 19 (2011) 4067–4074.

[26] S. Kotsovolou, A. Chiou, R. Verger, G. Kokotos, Bis-2-oxo amide triacylglycerol analogues: A novel class of potent human gastric lipase inhibitors, J. Org. Chem. 66 (2001) 962–967.

[27] A. Chiou, T. Markidis, V. Constantinou-Kokotou, R. Verger, G. Kokotos, Synthesis and study of a lipophilic α-keto amide inhibitor of pancreatic lipase, Org. Lett. 2 (2000) 347–350.

[28] G. Kokotos, R. Verger, A. Chiou, Synthesis of 2-oxo amide triacylglycerol analogues and study of their inhibition effect on pancreatic and gastric lipases, Chem. Eur. J. 6 (2000) 4211–4217.

[29] G. Moroy, V.Y. Martiny, P. Vayer, B.O. Villoutreix, M.A. Miteva, Toward *in silico* structure-based ADMET prediction in drug discovery, Drug Discov. Today. 17 (2012) 44-55.

[30] T.Y. Chen, M.M.C. Wang, S.K. Hsieh, M.H. Hsieh, W.Y. Chen, J.T.C. Tzen, Pancreatic lipase inhibition of strictinin isolated from Pu'er tea (*Camellia sinensis*) and its anti-obesity effects in C57BL6 mice, J. Funct. Foods. 48 (2018) 1–8.

[31] G. Avci, I. Küçükkurt, E. Küpeli Akkol, E. Yesilada, Effects of escin mixture from the seeds of *Aesculus hippocastanum* on obesity in mice fed a high fat diet, Pharm. Biol. 48 (2010) 247–252.